Intracellular Ca^{2+} and the phospholipid PIP_2 regulate the taste transduction ion channel TRPM5

Dan Liu and Emily R. Liman*

Department of Biological Sciences and Program in Neuroscience, University of Southern California, Los Angeles, CA 90089

Edited by Bertil Hille, University of Washington, Seattle, WA, and approved September 26, 2003 (received for review July 3, 2003)

The transduction of taste is a fundamental process that allows animals to discriminate nutritious from noxious substances. Three taste modalities, bitter, sweet, and amino acid, are mediated by G protein-coupled receptors that signal through a common transduction cascade: activation of phospholipase C $\beta 2$, leading to a breakdown of phosphatidylinositol-4,5-bisphosphate (PIP_2) into diacylglycerol and inositol 1,4,5-trisphosphate, which causes release of Ca^{2+} from intracellular stores. The ion channel, TRPM5, is an essential component of this cascade; however, the mechanism by which it is activated is not known. Here we show that heterologously expressed TRPM5 forms a cation channel that is directly activated by micromolar concentrations of intracellular Ca^{2+} ($K_{1/2}$ = 21 μM). Sustained exposure to Ca^{2+} desensitizes TRPM5 channels, but PIP_2 reverses desensitization, partially restoring channel activity. Whole-cell TRPM5 currents can be activated by intracellular Ca^{2+} and show strong outward rectification because of voltage-sensitive gating of the channels. TRPM5 channels are nonselective among monovalent cations and not detectably permeable to divalent cations. We propose that the regulation of TRPM5 by Ca^{2+} mediates sensory activation in the taste system.

Ion channels in the transient receptor potential (TRP) family conduct second messenger-gated currents that play diverse roles in cellular physiology. Many are known to mediate vertebrate and invertebrate sensory transduction, including visual transduction (1), pheromone detection (2–4), thermal reception (5–8), and mechanoreception (9, 10). TRP channels can be divided into three classes: TRPC, TRPV, and TRPM (11). Eight vertebrate TRP channels fall into the TRPM class on the basis of structural similarity to the founding member (melastatin) (12). Some of these channels are activated by varied stimuli, including ADP-ribose (TRPM2) (13, 14), Ca^{2+} (TRPM4) (15), and cold or menthol (TRPM8) (6, 7), whereas others are constitutively active (TRPM7) (16–18). Recently, a member of this family, TRPM5, was implicated in vertebrate taste transduction (19, 20); however, the mechanisms by which it is gated are not known.

The transduction of bitter, sweet, and amino acid tastes is mediated by G protein-coupled receptors that are distinct for each modality (reviewed in refs. 21 and 22). Although a variety of mechanisms have been proposed for taste transduction, recent evidence indicates that all three modalities use elements of a common pathway (20, 23); receptors signal through a heterotrimeric G protein to phospholipase C $\beta 2$ (PLC$\beta 2$), which breaks down phosphatidylinositol 4,5-bisphosphate (PIP_2) into inositol 1,4,5-trisphosphate (IP_3) and diacylglycerol (DAG), and IP_3 opens Ca^{2+}-release channels to elevate intracellular Ca^{2+}. Strong support for this pathway comes from a study of mice that carry a targeted deletion of PLC$\beta 2$ and are completely unresponsive to bitter, sweet, and amino acid tastes (20). In addition, it is known that taste cells respond to bitter and sweet stimuli with a rise in intracellular Ca^{2+} (24–26). Less understood is the mechanism by which this signaling pathway generates the electrical responses and changes in transmitter release that allow propagation of the signal through the nervous system. Two recent reports suggest that TRPM5 is a component of the channel that mediates transduction of this pathway (19, 20). TRPM5 is coexpressed in taste receptor neurons with G protein-coupled taste receptors (19, 20) and PLC$\beta 2$, and targeted deletion of TRPM5 in mice leads to the specific loss of taste sensitivity to bitter, sweet, and amino acids (20). Identification of the second messenger that activates TRPM5 will, thus, provide a framework with which to understand taste transduction. A recent study showed that depletion of Ca^{2+} stores by thapsigargin induced a current in TRPM5-expressing cells (19). However, a separate group reported instead that activation of TRPM5 is independent of release of Ca^{2+} from intracellular stores (20).

Here we show that TRPM5 forms a cation channel activated by micromolar concentrations of Ca^{2+}. After activation, TRPM5 channels undergo rapid Ca^{2+}-dependent desensitization, which is partially reversed by PIP_2. These data allow us to propose a model for taste transduction that links known receptor signaling events to membrane depolarization.

Methods

Molecular Cloning and Heterologous Expression. TRPM5 was amplified from mouse vomeronasal organ cDNA with plaque-forming unit DNA polymerase (Stratagene) as described (27) and was cloned into pBluescript KS+ (Stratagene). The coding sequence was identical to that previously reported (AAF98120) (28) except for a deletion of three nucleotides, resulting in the deletion of a threonine at position 130. The coding sequence was subcloned into pEGFP-C2 (Clontech) to generate an N-terminal fusion of enhanced GFP (EGFP) and into an EGFP dual promoter vector (pHGCX). Plasmid encoding TRPM5 was transiently transfected into cells [COS-7, Chinese hamster ovary (CHO)-K1, or HEK-293 M1, a cell line stably expressing the muscarinic M1 receptor (29)] by using Effectene (Qiagen, Valencia, CA) or Fugene (Roche Molecular Biochemicals) as suggested by the manufacturer. Transfected cells were identified by green fluorescence. Recordings were performed 24–72 h after transfection at room temperature.

Electrophysiology. All recording were made with an Axopatch 200B amplifier, digitized with a DIGIDATA 1322A, acquired with PCLAMP 8.2 and analyzed with CLAMPFIT 8.2 (Axon Instruments, Union City, CA). Records were sampled at 5 kHz and filtered at 1 kHz. For measurements of the voltage dependence of activation, series resistance compensation (85–95%) was used. Patch pipettes (1.5–3 Mohm) were fabricated from borosilicate glass. For excised patch recordings, pipettes were coated with Sylgard. Solution exchange was achieved by placing the patch or cell in front of a linear array of microperfusion pipes under computer control (Warner Instruments, Hamden, CT). For

This paper was submitted directly (Track II) to the PNAS office.

Abbreviations: TRP, transient receptor potential; PIP_2, phosphatidylinositol 4,5-bisphosphate; DAG, diacylglycerol; IP_3, inositol 1,4,5-trisphosphate; CHO, Chinese hamster ovary; OAG, oleoyl-2-acetyl-*sn*-glycerol; ACh, acetylcholine; PLC$\beta 2$, phospholipase C $\beta 2$; eGFP, enhanced GFP.

*To whom correspondence should be addressed at: Department of Biological Sciences, 3641 Watt Way, Los Angeles, CA 90089-2520. E-mail: liman@usc.edu.

www.pnas.org/cgi/doi/10.1073/pnas.2334159100

whole-cell recording of ion selectivity and block, solutions were exchanged every 2 s, and responses were compared with control responses before and after solution exchange.

All solutions were pH 7.4 and were adjusted to 290–310 mosmol with sucrose. Solutions were as follows. For perforated-patch recording, the pipette solution was 140 mM CsCl/5 mM 1,2-bis(2-aminophenoxy)ethane-*N,N,N',N'*-tetraacetic acid (BAPTA)/3.8 mM $CaCl_2$/1 mM $MgCl_2$/10 mM Hepes/16 μg/ml amphotericin. Extracellular solution was 150 mM NaCl/2 or 10 mM $CaCl_2$/10 mM Hepes. For whole-cell recording of receptor-operated currents, the intracellular solution was 140 mM CsCl/2 mM $MgCl_2$/2 mM NaATP/10 mM Hepes (10 mM EGTA was added to block Ca^{2+} signaling in some experiments). For whole-cell recording of Ca^{2+}-activated currents, the intracellular solution was 140 mM CsCl/2 mM MgATP/10 mM Hepes/2 mM *N*-(2-hydroxyethyl)ethylene-diaminetriacetic acid (HEDTA)/1.5 mM $CaCl_2$ (40 μM free Ca^2). For selectivity experiments, the extracellular solution contained 10 mM Hepes and 145 mM NaCl, 145 mM CsCl, or 145 mM KCl. For determination of Ca^{2+} permeability, the external solution contained 10 mM Hepes and 50 mM $CaCl_2$, 90 mM *N*-methyl-D-glucamine (NMDG), or 2 mM $CaCl_2$ and 160 mM NMDGCl. For all other whole-cell experiments, the external solution contained 145 mM NaCl, 10 mM Hepes, and 2 mM $CaCl_2$. For excised patch recording the pipette contained 150 mM NaCl, 10 mM Hepes, 2 mM EGTA, and 1.8 mM $CaCl_2$ (≈500 nM free Ca^{2+}; the low Ca^{2+} solution was not important for these recordings). Immediately after seal formation and before excision, the external solution was replaced with a 0 Ca^{2+} solution: 150 mM NaCl/10 mM Hepes/2 mM HEDTA. Solutions with micromolar concentrations of free Ca^{2+} were obtained by adding Ca^{2+} to this HEDTA-based solution as follows: 0.5 mM $CaCl_2$ for 1 μM free Ca^{2+}, 1.2 mM $CaCl_2$ for 5 μM free Ca^{2+}, 1.6 mM $CaCl_2$ for 12 μM free Ca^{2+}, and 1.9 mM $CaCl_2$ for 40 μM free Ca^{2+}. Solutions containing 100 and 500 μM Ca^{2+} were made by adding 0.1 and 0.5 mM $CaCl_2$ to 150 mM NaCl/10 mM Hepes. All Ca^{2+} concentrations are reported as calculated with MAXCHELATOR (www.stanford.edu/~cpatton/maxc.html) and were confirmed by direct measurement with a Ca^{2+}-sensitive electroprobe (Microelectrodes, Bedford, NH). Concentrations of drugs were as follows: 10 or 20 μM 4-bromo A23187 (Molecular Probes)/10 μM diC8-PIP_2 (Echelon Bioscience, Salt Lake City)/1:200 anti-PIP_2 antibody (Echelon Bioscience and Assay Designs, Ann Arbor, MI), 100 μM 1-oleoyl-2-acetyl-*sn*-gylcerol (OAG) (Avanti Polar Lipids, Alabaster, AL), 10 μM IP_3 (Research Biochemicals International, Natick, MA), 50 μM calmidizolium (Calbiochem), 5 μM thapsigargin (Calbiochem), and 20 μM U73122 (Calbiochem).

Data Analysis. All data were analyzed by CLAMPFIT (Axon Instruments) and curve fitting and statistical analyses were done in Origin (Microcal, Northampton, MA). For excised patches, we classified recordings according to whether the patch was desensitized and grouped data before analysis. This was necessary because occasionally a patch was inadvertently exposed to Ca^{2+} before running the stimulus protocol. For each experiment, we determined the ratio of current evoked by 12 and 40 μM Ca^{2+}; this ratio was 0.22 ± 0.02 (n = 21) for the first recording and 0.05 ± 0.01 (n = 9) in patches that were desensitized intentionally. If the ratio was <0.10, the patch was considered desensitized. Leak current in excised patches was determined from the magnitude of the current in 0 Ca^{2+} before and after each stimulus application. Capacitive current was subtracted from whole-cell I–V curves. Permeability ratios of monovalent cations with respect to the permeability of Cs^+ were determined from the equation $P_x/P_{Cs} = \exp(F/RT\Delta E_{rev})$, where ΔE_{rev} is the change in reversal potential in switching from Cs^+ containing external solution to an external solution with an equal concentration of cation x. Measured liquid junction potentials for all solutions were <3 mV and were not corrected. Dose–response curves were fit with a Hill equation of the form $y = V_{max}(x^n/(k^n + x^n))$. All data are presented as mean ± SEM.

Results

TRPM5 Forms a Ca^{2+}-Activated Channel. To determine possible mechanisms by which taste transduction leads to activation of TRPM5 channels, we performed patch clamp recording from CHO-K1 cells transfected with TRPM5. An N-terminal GFP-tagged TRPM5 construct (referred to as TRPM5) was generated to allow identification of cells expressing the TRPM5 protein. To test for second messenger activation of TRPM5 channels, we excised patches from transfected cells and exposed them to three putative second messengers: DAG, IP_3, or Ca^{2+}. As can be seen in Fig. 1*a*, 40 μM Ca^{2+} reproducibly elicited a current, whereas no current was elicited in response to either OAG (an analog of DAG, 100 μM, n = 10), which has been shown to be an activator of some TRPC channels (30), or IP_3 (10 μM, n = 10). The mean current elicited on initial exposure to 40 μM Ca^{2+} was −26.5 ± 6.9 pA (−80 mV) in patches from transfected cells (n = 27); this was significantly greater than the current evoked in patches from untransfected cells (−4.1 ± 2.1 pA, n = 12, $P < 0.05$, Student's t test).

Ca^{2+} exposure produced flickery openings of single TRPM5 channels, with a slope conductance of 16 pS (n = 3; Fig. 1*b*). This conductance is further confirmed by analysis of TRPM5 channel activity at −80 mV, which reveals a unitary current of 1.2 ± 0.1 pA (n = 6), corresponding to a unitary chord conductance of 15 ± 1 pS. A reversal potential of 0 mV was assumed, based on analysis of whole-cell currents (see below). At high Ca^{2+} concentrations (>100 μM), an endogenous channel could be activated in CHO-K1 cells (1/12 patches). In addition to its lower sensitivity to Ca^{2+}, this channel could be clearly distinguished from TRPM5 channels on the basis of its larger conductance (≈25 pS) and long openings (data not shown). Patches that showed this channel activity were not used for further analysis.

We quantified the sensitivity of TRPM5 channels in response to Ca^{2+} concentrations ranging from 5 to 500 μM (Fig. 1*c*). In patches that had not been previously exposed to Ca^{2+}, dose–response relations could be fit with a $K_{1/2}$ of 21.5 ± 1.8 μM and a Hill coefficient of 2.4 ± 0.2 (n = 3; Fig. 1*d*). In performing these experiments, we noted that the sensitivity of the channel to Ca^{2+} varied according to whether the patch had previously been exposed to Ca^{2+}. Indeed, as shown in Fig. 1 *c* and *d*, repeated application of a dose–response protocol led to a reduction in the peak amplitude of the current as well as a change in the sensitivity of the current to Ca^{2+}. The shift in the dose–response relation stabilized after repeated exposure to Ca^{2+}. After desensitization, the current in response to 40 μM Ca^{2+} was reduced to 8 ± 2% of its initial magnitude (n = 7). Assuming no change in the shape of the dose–response relation, our data are consistent with an ≈4-fold reduction in sensitivity to Ca^{2+}, and an ≈4-fold reduction in the peak amplitude (Fig. 1*d*).

Desensitization of TRPM5 Is Ca^{2+}-Dependent. Desensitization of TRPM5 channels could be caused by a steady loss of a signaling molecule after patch excision or by a process that is specifically stimulated by Ca^{2+}. To distinguish between these possibilities, we repeatedly elicited TRPM5 currents by application of 40 μM intracellular Ca^{2+} and intermittently exposed patches to 500 μM Ca^{2+}. A gradual decline in the current was observed in response to application of 40 μM Ca^{2+}, whereas activation of the current by 500 μM Ca^{2+} led to a dramatic reduction in the current (Fig. 2*a*), indicating that the decline in the current is caused by a Ca^{2+}-dependent process. To confirm this result, we measured the response of TRPM5 currents to prolonged Ca^{2+} exposure (Fig. 2*b*). TRPM5 currents decayed with a time course that could

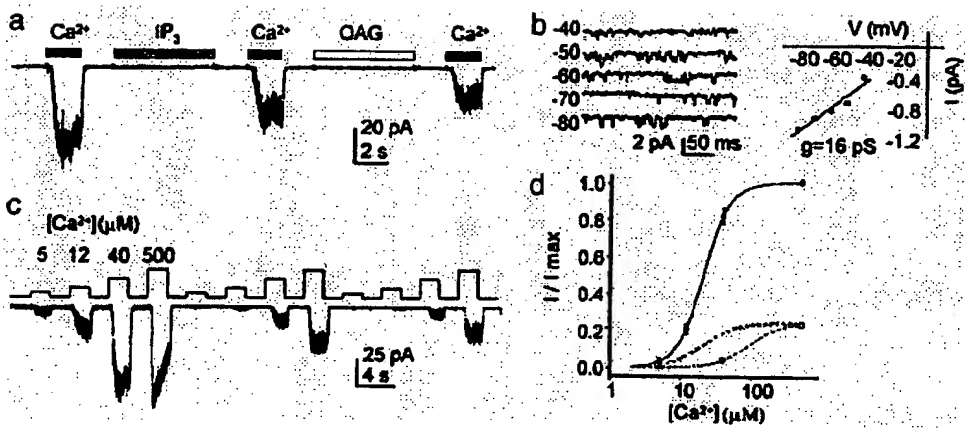

Fig. 1. TRPM5 is activated by micromolar concentrations of Ca^{2+}. (*a*) Activation by 40 μM Ca^{2+} of an inward current in a patch excised from a TRPM5-transfected CHO-K1 cell (V_m = −80 mV). Neither 10 μM IP_3 nor 100 μM OAG elicited a current in the same patch. (*b*) Single-channel recording at different voltages in response to 12 μM Ca^{2+} (*Left*). The I–V relation of the same patch (*Right*) yields a slope conductance of 16 pS. No channel activity was seen in this patch in the absence of Ca^{2+}. (*c*) Responses of TRPM5 channels to increasing concentrations of Ca^{2+}. Note the desensitization of the channels in response to repeated application of the stimulus protocol. (*d*) Dose–response relations from patches (V_m = −80 mV) before (filled circles) or after (open circles) desensitization (mean ± SEM, n = 3 patches; data were normalized to the peak current in each patch). Fits are to the Hill equation with $K_{1/2}$ = 21 μM, n = 2.4, and V_{max} = 1.05 before desensitization (solid line) and $K_{1/2}$ = 77 μM, n = 2.4, and V_{max} = 0.23 after desensitization (dashed line; note this fit was obtained by holding n constant, but allowing V_{max} and $K_{1/2}$ to vary). The dotted line shows the predicted relationship if only the maximum current were to decline (simulation with $K_{1/2}$ = 21 μM, n = 2.4, and V_{max} = 0.23), illustrating that with desensitization the dose–response relationship shows a shift in sensitivity as well as a decrease in the maximal current activated.

be fit with a single exponential and the rate of decay was linearly related to the concentration of Ca^{2+}, indicating that Ca^{2+} mediates desensitization (Fig. 2*c*). A number of TRP channels show inactivation or desensitization in response to entry of extracellular Ca^{2+} (e.g., refs. 6 and 31). For the *Drosophila* light-activated channel TRPl, Ca^{2+}-dependent inactivation appears to be mediated by calmodulin, which directly binds to the channel (32). We were unable to block desensitization or activation of TRPM5 currents by the calmodulin inhibitor calmidizolium (50 μM; n = 4), although this does not rule out a role for calmodulin in either of these processes.

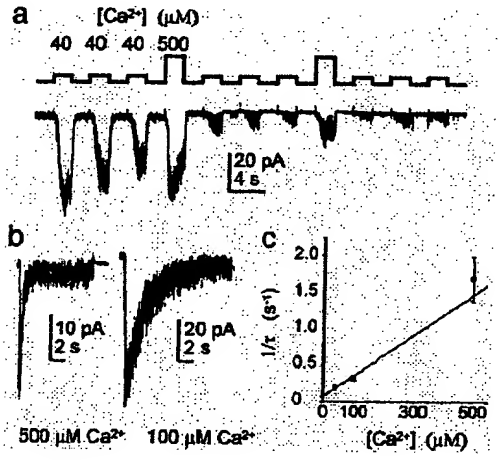

Fig. 2. Desensitization of TPRM5 is Ca^{2+}-dependent. (*a*) Responses in an excised patch (−80 mV) to repeated applications of Ca^{2+}. Note that the current declined gradually in response to repeated exposures to 40 μM Ca^{2+} but declined dramatically in response to 500 μM Ca^{2+}. (*b*) Response in patches to prolonged exposure to Ca^{2+} (−80 mV). Single exponential fits are shown in red. (*c*) The rate of decay of the current ($1/\tau$) is linearly related to Ca^{2+} concentration, over the range measured, indicating that desensitization is Ca^{2+}-dependent (mean ± SEM, n = 5 patches for each data point).

Desensitization of TRPM5 Is Partially Reversed by PIP_2. These data suggest that, in response to a prolonged increase in intracellular Ca^{2+}, TRPM5 channels will desensitize. What is the mechanism by which the sensitivity of the channels is then restored? We reasoned that because levels of PIP_2 are depleted during PLC signaling and restored after termination of PLC signaling (18, 33–35), PIP_2 might act to restore the sensitivity of TRPM5 channels. To test this hypothesis, we used a short chain synthetic PIP_2, $DiC_8PI(4,5)P_2$, hereafter referred to as PIP_2. Application of PIP_2 alone did not elicit any current in patches excised from TRPM5-expressing cells (n = 3), and, before desensitization of the channels, PIP_2 had no effect on the magnitude of the current elicited by a range of Ca^{2+} concentrations (Fig. 3 *a* and *b*; for 40 μM Ca^{2+}, $P > 0.05$, paired t test). In contrast, after desensitization, application of 10 μM PIP_2 led to a dramatic enhancement of the current in response to Ca^{2+} (Fig. 3*a*). In these experiments, the response to a 2-s application of 40 μM Ca^{2+} was enhanced ≈4-fold when PIP_2 and Ca^{2+} were applied together (Fig. 3*b*; $P < 0.01$, paired t test). Longer application of PIP_2 led to slightly larger enhancement of the current, with a maximal effect reached after ≈6 s. Dose–response relations, measured from desensitized channels in the absence or presence of PIP_2, showed that PIP_2 partially restored the sensitivity of the channel to Ca^{2+} (Fig. 3*c*). Neither application of IP_3 (n = 4) nor application of OAG (n = 4) led to any change in the magnitude of the current after desensitization.

The observation that PIP_2 enhances TRPM5 currents only after they have desensitized suggests that desensitization may involve the loss of bound PIP_2 through a Ca^{2+}-dependent mechanism. One possibility is that Ca^{2+} activates native phospholipases (36), and that this leads to a depletion of PIP_2 in the patch. However, application of neither the PLC inhibitor U73122 (20 μM; n = 8) nor IP_3 (10 μM; n = 6) (which can displace PIP_2 from the binding site of some PLCs) changed the rate or extent of Ca^{2+}-dependent desensitization. We were also unable to promote desensitization through application of two different anti-PIP_2 antibodies, suggesting that if PIP_2 is bound to the channel, it is not readily accessible.

Whole-Cell TRPM5 Currents in Response to Elevation of Intracellular Ca^{2+} by Ionophore and G Protein-Coupled Receptor Signaling. To confirm results obtained from excised patches and to study the

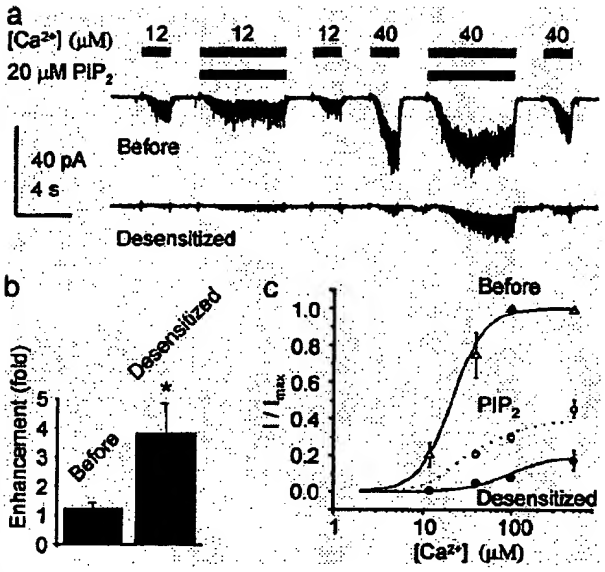

Fig. 3. PIP_2 partially restores TRPM5 channel activity after desensitization. (*a*) Responses to 12 and 40 μM Ca^{2+} in the presence and absence of 20 μM PIP_2 before and after desensitization. Desensitization was induced by a 30-s exposure to 40 μM Ca^{2+} (V_m = −80 mV). PIP_2 enhances the current in response to Ca^{2+} after, but not before, desensitization. (*b*) Enhancement of the current in response to 40 μM Ca^{2+} by PIP_2 before (n = 6) and after desensitization (n = 8). Current amplitudes are the averaged peak magnitude recorded within 2 s from the start of Ca^{2+} exposure. The asterisk indicates that the difference between the enhancement of control and desensitized currents was significant at $P < 0.05$. (*c*) Dose–response relations before desensitization (open triangles), after desensitization (filled circles), and after desensitization in the presence of 10 μM PIP_2 (open circles) (mean ± SEM, n = 3 patches). In these experiments, PIP_2 was present before and during a 6-s application of Ca^{2+}. Currents are normalized to the maximum current obtained in each patch. Solid lines are the same fits as in Fig. 1*d*. The dashed line shows the expected relationship if 25% of the current recovered full sensitivity. The data could not be well fitted by assuming that either only the maximum current or the sensitivity was restored by PIP_2.

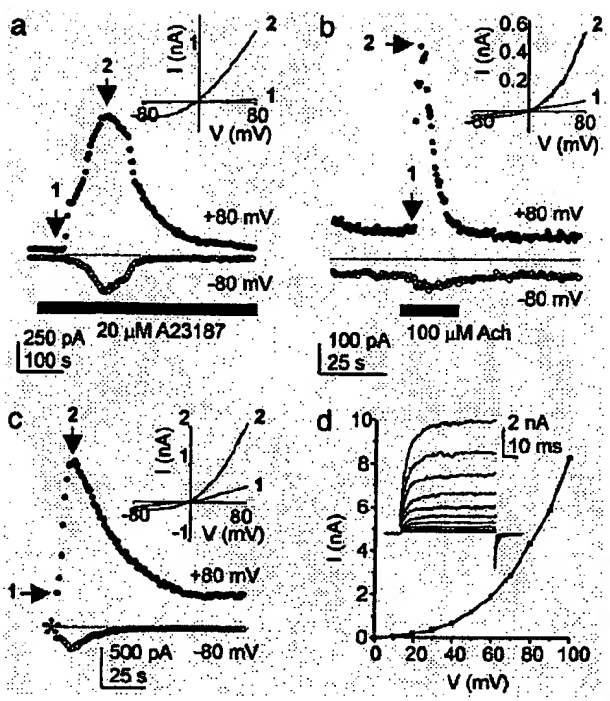

Fig. 4. Electrophysiological properties of TRPM5 expressed in HEK-293 M1 cells. (*a*) Application of the Ca^{2+} ionophore A23187 (20 μM) in the presence of 2 mM extracellular Ca^{2+} in perforated-patch recording mode elicits a large outwardly rectifying current. (*Inset*) The current in response to a ramp depolarization (1 V/s) at the times indicated. (*b*) Application of ACh (100 μM) induced a transient current in HEK-293 M1 cells cotransfected with TRPM5 and G16z44. (*Inset*) The current in response to a ramp depolarization (0.44 V/s) at the times indicated. The pipette solution contained no Ca^{2+} buffer. (*c*) In whole-cell recording mode, 40 μM Ca^{2+} in the pipette elicited a large rectifying current. Recording began shortly after break into the whole-cell mode. (*Inset*) The current in response to a ramp depolarization (1 V/s). (*d*) Currents in response to a family of step depolarizations and the resulting I–V relationship for the peak current at each voltage. Steps are to 0–100 mV from a holding potential of −80 mV with repolarization to −50 mV. Note the prominent relaxation of the current upon depolarization, consistent with voltage-dependent gating of the channels. A small fraction of the current showed a fast increase, indicating that there is low, but nonzero, probability of opening at the resting potential (−80 mV).

properties of TRPM5 currents in more detail, we measured electrical responses in whole-cell recording mode from HEK-293 M1 cells transfected with TRPM5. Perforated-patch recording was used in initial experiments to maintain intracellular signaling components intact. Upon attaining electrical access, little current was present in transfected cells, indicating that TRPM5 is not constitutively active (Fig. 4*a*). Introduction of the membrane-permeant Ca^{2+} ionophore A23187 in the presence of 2 mM Ca^{2+} induced a large outwardly rectifying current in TRPM5-expressing cells (Fig. 4*a*). In total, 12 of 14 TRPM5-transfected cells responded to the Ca^{2+} ionophore (peak induced I = 547 ± 140 pA at +80 mV and −182 ± 62 pA at −80 mV, n = 14), whereas none of the untransfected cells responded to the Ca^{2+} ionophore (peak induced I = 7.5 ± 4 pA at +80 mV and 0 ± 1 pA at −80, n = 7, $P < 0.01$). Rundown of the TRPM5 current was consistently observed in these recordings and is reminiscent of the Ca^{2+}-induced desensitization of channels observed in excised patches

To determine whether TRPM5 currents can be activated downstream of a G protein-coupled receptor, we measured electrical responses in HEK-293 M1 cells transfected with TRPM5 to stimulation with acetylcholine (ACh). The M1 muscarinic ACh receptor expressed by these cells couples to PLC (29), leading to PIP_2 hydrolysis and Ca^{2+} elevation. To improve coupling of the M1 receptor to native PLCs, we cotransfected the chimeric G protein, G16z44 (37). In whole-cell recording, with no Ca^{2+} buffer in the pipette, we observed a large outwardly rectifying current in response to application of 100 μM ACh (two of three cells responded, Fig. 4*b*). In contrast, we did not observe activation of a current in response to ACh when the patch pipette contained a Ca^{2+} buffer, EGTA (10 mM; n = 3). These data suggest that physiological concentrations of Ca^{2+} elicited by stimulation of a G protein-coupled receptor that couples to PLC can activate TRPM5.

Ion Selectivity and Voltage-Sensitive Gating of TRPM5. Ion selectivity of TRPM5 channels was assessed in whole-cell recordings from HEK-293 M1 cells. Intracellular dialysis of 40 μM Ca^{2+} rapidly induced a large outwardly rectifying current in cells transfected with TRPM5 (peak I = 2.58 ± 0.43 nA at +80 mV, n = 16) but not in untransfected cells (peak I = 0.19 ± 0.07 nA, n = 7, $P <$ 0.01; Fig. 4*c*) Large outwardly rectifying currents were also observed in response to intracellular dialysis of Ca^{2+} in CHO-K1 and COS-7 cells transfected with TRPM5 and in HEK-293 M1 cells transfected with a TRPM5 construct that was not fused to GFP (data not shown). In whole-cell recording, as in perforated-

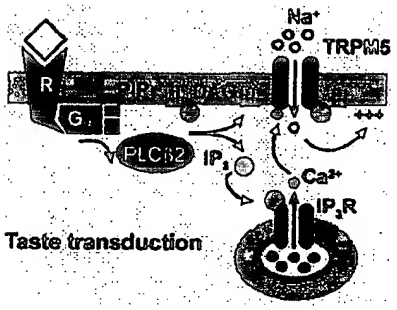

Fig. 5. A model for taste transduction. Binding of taste stimuli to G protein-coupled taste receptors (R) leads to dissociation of the heterotrimeric G protein. $\beta\gamma$ subunits of the G protein activate PLCβ2, which in turn hydrolyzes PIP_2 into DAG and IP_3. IP_3 activates IP_3 receptors, which release Ca^{2+} from intracellular stores. Intracellular Ca^{2+} opens TRPM5 channels, leading to an influx of Na^+ and depolarization of the cell. Note that TRPM5 is not permeable to Ca^{2+} and, therefore, there is no positive feedback loop.

patch recording, the TRPM5 current inactivated over the time course of tens of seconds (Fig. 4c). Ion substitution experiments revealed that TRPM5 is equally permeable to K^+, Na^+, and Cs^+ ($P_{Na}/P_{Cs} = 1.1$, $P_K/P_{Cs} = 1.2$, $n = 5$; Fig. 6, which is published as supporting information on the PNAS web site). We did not detect any permeability to Ca^{2+} ($E_{rev} = -43.6 \pm 3.4$ mV in 50 mM Ca^{2+}, 90 mM $NMDG^+$ as compared with $E_{rev} = -44.2 \pm 3.9$ mV in 2 mM Ca^{2+}, 160 $NMDG^+$; $n = 5$). Removal of external Ca^{2+} (with EGTA), external Mg^{2+} (with EDTA), or both (with EDTA) did not lead to a significant increase in the magnitude of the inward current or to a change in the rectification of the current ($n = 4$), indicating that TRPM5 channels are not blocked by divalent cations. We also did not observe any block of TRPM5 currents by La^{3+} (200 μM, $n = 4$).

The pronounced rectification of TRPM5 currents could be due to an inherent voltage sensitivity of the channels. Indeed, whole-cell currents in HEK-293 M1 cells expressing TRPM5 evoked in response to intracellular dialysis of 40 μM Ca^{2+} showed a clear relaxation to a higher current level with depolarizing voltage steps (Fig. 4d; similar results were obtained in 5 cells). Voltage-sensitive gating has also been observed for TRPM8 and TRPM4 currents (6, 38). A comparison of the fourth transmembrane domain (S4) of TRPM5, TRPM4, and TRPM8 with that of voltage-sensitive K^+ channels shows a striking similarity, suggesting that similar structural elements underlie voltage-dependent gating in these disparate channels (39). For any of the TRP channels, the physiological significance of this additional level of regulation is not known.

Discussion

Our data show that TRPM5, which is essential for taste transduction (20), forms a nonselective cation channel that is directly gated by micromolar concentrations of Ca^{2+}. In addition, we show that TRPM5 is regulated by PIP_2, which enhances sensitivity of the channels to Ca^{2+}. These data support a model for sensory transduction of bitter, sweet, and amino acid stimuli in taste cells, shown in Fig. 5. In this model, taste receptors signal through PLCβ2 to release Ca^{2+} from intracellular stores, which rapidly activates TRPM5 channels. This is consistent with physiological data and with results from targeted deletion of taste transduction molecules. (20, 23–26, 40–42)

Mechanism of TRPM5 Activation. The mechanism of activation of TRPM5 has been controversial, with conflicting data published in two previous reports (19, 20). Although there is general agreement that TRPM5 is activated downstream of PLC, the nature of the second messenger that activates TRPM5 has eluded previous investigations. One report showed that prolonged treatment with thapsigargin, which inhibits uptake of Ca^{2+} into intracellular stores, leads to the development of a linear conductance in TRPM5-expressing cells (19). These data were used to argue that TRPM5 is activated by depletion of Ca^{2+} stores. The conductance described in this report does not resemble the TRPM5 currents that we recorded, either in rectification properties, Ca^{2+} permeability, or sensitivity to La^{3+} block. Furthermore, we were unable to observe significant activation of TRPM5 by short-term thapsigargin treatment, presumably because of the relatively slow elevation of intracellular Ca^{2+} (Fig. 7, which is published as supporting information on the PNAS web site). A second study showed that G protein-coupled receptors could activate TRPM5 currents, but that the response was not occluded when intracellular Ca^{2+} was heavily buffered (19). These results were used to argue that TRPM5 activation is independent of release of Ca^{2+} from intracellular stores. In similar experiments, we found that TRPM5 currents could be activated downstream of a G protein-coupled receptor; however, we failed to observe activation of this current if the intracellular pipette solution contained a Ca^{2+} buffer. Importantly, neither previous study directly tested whether Ca^{2+} activates TRPM5 channels. By using excised patch and whole-cell recording, we directly demonstrate that TRPM5 is Ca^{2+}-activated. Similar results were recently obtained by Hofmann *et al.* (43).

Ca^{2+} levels in taste cells in response to taste stimuli reach only high nanomolar levels (24–26); however, we report that TRPM5 has micromolar sensitivity to Ca^{2+}, a result that might appear incompatible with an essential role of TRPM5 in taste transduction (20). However, as noted by the authors of one of these studies, these measurements underestimate true Ca^{2+} levels because of spatial and temporal averaging (25). In restricted microdomains of cells, Ca^{2+} levels can reach low micromolar concentrations (44), which would be sufficient to activate a TRPM5 current. It will be interesting to determine whether TRPM5 channels are localized in taste cells in proximity to sites of Ca^{2+} release or entry, as might be expected if they are to be efficiently gated by Ca^{2+}. An alternative explanation for this apparent discrepancy is that TRPM5 forms a heteromultimer with other channel subunits in taste cells, leading to an alteration in Ca^{2+} sensitivity. Study of native Ca^{2+}-activated nonselective channels from taste cells will be needed to address this possibility.

Our study raises a number of questions concerning the mechanisms of activation and inactivation of TRPM5. The Ca^{2+} dependence of activation may be conferred on the channel by auxiliary subunits, such as calmodulin, as is the case for small conductance Ca^{2+}-activated K^+ channels (45) or it may be an inherent property of the channel, as is the case for large conductance Ca^{2+}- and voltage-activated K^+ channels (46). Ca^{2+}-depedendent desensitization may similarly involve direct binding of Ca^{2+} to the channel or may be mediated by associated or nonassociated proteins. One attractive model is that Ca^{2+} induces an allosteric change in the TRPM5 protein that lowers its affinity for PIP_2. We cannot rule out the possibility that desensitization of the channel is independent of PIP_2 binding, and that the desensitized channel is more sensitive to PIP_2 modulation.

A Molecular Basis for Ca^{2+}-Activated Nonselective Cation Channels. Ca^{2+}-activated nonselective cation channels have been described in a large number of cell types (47); however, their physiological functions are not well understood and their molecular identity remains obscure. A previous report demonstrated that a related channel, TRPM4, encodes a Ca^{2+}-activated cation channel with sensitivity to Ca^{2+} in the high nanomolar range (ref. 15, but see

also ref. 38). Our data show that TRPM5 also encodes a Ca^{2+}-activated nonselective ion channel. In addition to lingual epithelium, TRPM5 is detected in stomach, intestine, uterus, and testis (19), and it is likely that on closer examination it will be found in other tissues and cell types. We cloned TRPM5 from the vomeronasal sensory epithelium, where it shows low levels of expression (D.L. and E.R.L., unpublished data). TRPM5 does not match properties of Ca^{2+}-activated nonselective channels that have been described in vomeronasal sensory neurons (48), suggesting that it might form a heteromultimer with additional subunits.

TRPs and PIPs. PIP_2, once regarded simply as the substrate from which second messengers are generated, has recently been shown to be an important regulator of transporters and ion channels, including several TRP channels (18, 49, 50). PIP_2 inhibits gating of TRPV1, and receptor-stimulated hydrolysis of PIP_2 relieves the channel from inhibition leading to a lower threshold for activation by protons, capsaicin, and heat (49, 50). For TRPM5, PIP_2 appears to play an opposite role in modulating channel activity: PIP_2 promotes gating of TRPM5 channels, which, after desensitization, are activated by lower concentrations of Ca^{2+} in the presence of PIP_2. Similarly, PIP_2 promotes gating of TRPM7, which is constitutively active and inactivated by PIP_2 hydrolysis (18). Our *in vitro* data suggest that PIP_2 might play a significant role in modulation of taste transduction. Further defining that role should be a major goal of future studies.

Note Added in Proof. After acceptance of our manuscript, we learned about a complementary paper (51) published in this issue. The main results and conclusions of that study also support the notion that TRPM5 indeed represents an intracellular Ca^{2+}-activated cation channel.

We thank T. Zhu for expert technical assistance, D. Arnold, L. Byerly, and L. Runnels for helpful discussion, and D. Arnold, L. Byerly, K.-W. Yau, and R. Kramer for critically reading the manuscript. This work was supported by National Institutes of Health Grants R01DC04213 and K02DC05000 and by the program for Women in Science and Engineering at the University of Southern California.

1. Hardie, R. C. & Raghu, P. (2001) *Nature* **413**, 186–193.
2. Liman, E. R., Corey, D. P. & Dulac, C. (1999) *Proc. Natl. Acad. Sci. USA* **96**, 5791–5796.
3. Stowers, L., Holy, T. E., Meister, M., Dulac, C. & Koentges, G. (2002) *Science* **295**, 1493–1500.
4. Leypold, B. G., Yu, C. R., Leinders-Zufall, T., Kim, M. M., Zufall, F. & Axel, R. (2002) *Proc. Natl. Acad. Sci. USA* **99**, 6376–6381.
5. Caterina, M. J., Schumacher, M. A., Tominaga, M., Rosen, T. A., Levine, J. D. & Julius, D. (1997) *Nature* **389**, 816–824.
6. McKemy, D. D., Neuhausser, W. M. & Julius, D. (2002) *Nature* **416**, 52–58.
7. Peier, A. M., Moqrich, A., Hergarden, A. C., Reeve, A. J., Andersson, D. A., Story, G. M., Earley, T. J., Dragoni, I., McIntyre, P., Bevan, S. & Patapoutian, A. (2002) *Cell* **108**, 705–715.
8. Benham, C. D., Gunthorpe, M. J. & Davis, J. B. (2003) *Cell Calcium* **33**, 479–487.
9. Colbert, H. A., Smith, T. L. & Bargmann, C. I. (1997) *J. Neurosci.* **17**, 8259–8269.
10. Walker, R. G., Willingham, A. T. & Zuker, C. S. (2000) *Science* **287**, 2229–2234.
11. Montell, C., Birnbaumer, L., Flockerzi, V., Bindels, R. J., Bruford, E. A., Caterina, M. J., Clapham, D. E., Harteneck, C., Heller, S., Julius, D., *et al.* (2002) *Mol. Cell* **9**, 229–231.
12. Hunter, J. J., Shao, J., Smutko, J. S., Dussault, B. J., Nagle, D. L., Woolf, E. A., Holmgren, L. M., Moore, K. J. & Shyjan, A. W. (1998) *Genomics* **54**, 116–123.
13. Perraud, A. L., Fleig, A., Dunn, C. A., Bagley, L. A., Launay, P., Schmitz, C., Stokes, A. J., Zhu, Q., Bessman, M. J., Penner, R., *et al.* (2001) *Nature* **411**, 595–599.
14. Sano, Y., Inamura, K., Miyake, A., Mochizuki, S., Yokoi, H., Matsushime, H. & Furuichi, K. (2001) *Science* **293**, 1327–1330.
15. Launay, P., Fleig, A., Perraud, A. L., Scharenberg, A. M., Penner, R. & Kinet, J. P. (2002) *Cell* **109**, 397–407.
16. Nadler, M. J., Hermosura, M. C., Inabe, K., Perraud, A. L., Zhu, Q., Stokes, A. J., Kurosaki, T., Kinet, J. P., Penner, R., Scharenberg, A. M. & Fleig, A. (2001) *Nature* **411**, 590–595.
17. Runnels, L. W., Yue, L. & Clapham, D. E. (2001) *Science* **291**, 1043–1047.
18. Runnels, L. W., Yue, L. & Clapham, D. E. (2002) *Nat. Cell Biol.* **4**, 329–336.
19. Perez, C. A., Huang, L., Rong, M., Kozak, J. A., Preuss, A. K., Zhang, H., Max, M. & Margolskee, R. F. (2002) *Nat. Neurosci.* **5**, 1169–1176.
20. Zhang, Y., Hoon, M. A., Chandrashekar, J., Mueller, K. L., Cook, B., Wu, D., Zuker, C. S. & Ryba, N. J. (2003) *Cell* **112**, 293–301.
21. Margolskee, R. F. (2002) *J. Biol. Chem.* **277**, 1–4.
22. Lindemann, B. (2001) *Nature* **413**, 219–225.
23. Wong, G. T., Gannon, K. S. & Margolskee, R. F. (1996) *Nature* **381**, 796–800.
24. Akabas, M. H., Dodd, J. & Al-Awqati, Q. (1988) *Science* **242**, 1047–1050.
25. Bernhardt, S. J., Naim, M., Zehavi, U. & Lindemann, B. (1996) *J. Physiol.* **490**, 325–336.
26. Ogura, T., Mackay-Sim, A. & Kinnamon, S. C. (1997) *J. Neurosci.* **17**, 3580–3587.
27. Liman, E. R. & Buck, L. B. (1994) *Neuron* **13**, 611–621.
28. Enklaar, T., Esswein, M., Oswald, M., Hilbert, K., Winterpacht, A., Higgins, M., Zabel, B. & Prawitt, D. (2000) *Genomics* **67**, 179–187.
29. Peralta, E. G., Ashkenazi, A., Winslow, J. W., Ramachandran, J. & Capon, D. J. (1988) *Nature* **334**, 434–437.
30. Hofmann, T., Obukhov, A. G., Schaefer, M., Harteneck, C., Gudermann, T. & Schultz, G. (1999) *Nature* **397**, 259–263.
31. Hardie, R. C. & Minke, B. (1994) *J. Gen. Physiol.* **103**, 409–427.
32. Phillips, A. M., Bull, A. & Kelly, L. E. (1992) *Neuron* **8**, 631–642.
33. Hardie, R. C., Raghu, P., Moore, S., Juusola, M., Baines, R. A. & Sweeney, S. T. (2001) *Neuron* **30**, 149–159.
34. Suh, B. C. & Hille, B. (2002) *Neuron* **35**, 507–520.
35. Zhang, H., Craciun, L. C., Mirshahi, T., Rohacs, T., Lopes, C. M., Jin, T. & Logothetis, D. E. (2003) *Neuron* **37**, 963–975.
36. Varnai, P. & Balla, T. (1998) *J. Cell Biol.* **143**, 501–510.
37. Mody, S. M., Ho, M. K., Joshi, S. A. & Wong, Y. H. (2000) *Mol. Pharmacol.* **57**, 13–23.
38. Nilius, B., Prenen, J., Droogmans, G., Voets, T., Vennekens, R., Freichel, M., Wissenbach, U. & Flockerzi, V. (2003) *J. Biol. Chem.* **278**, 30813–30820.
39. Jiang, Y., Lee, A., Chen, J., Ruta, V., Cadene, M., Chait, B. T. & MacKinnon, R. (2003) *Nature* **423**, 33–41.
40. Hwang, P. M., Verma, A., Bredt, D. S. & Snyder, S. H. (1990) *Proc. Natl. Acad. Sci. USA* **87**, 7395–7399.
41. Huang, L., Shanker, Y. G., Dubauskaite, J., Zheng, J. Z., Yan, W., Rosenzweig, S., Spielman, A. I., Max, M. & Margolskee, R. F. (1999) *Nat. Neurosci.* **2**, 1055–1062.
42. Ogura, T., Margolskee, R. F. & Kinnamon, S. C. (2002) *J. Neurophysiol.* **87**, 3152–3155.
43. Hofmann, T., Chubanov, V., Gudermann, T. & Montell, C. (2003) *Curr. Biol.* **13**, 1153–1158.
44. Neher, E. (1998) *Neuron* **20**, 389–399.
45. Xia, X. M., Fakler, B., Rivard, A., Wayman, G., Johnson-Pais, T., Keen, J. E., Ishii, T., Hirschberg, B., Bond, C. T., Lutsenko, S., *et al.* (1998) *Nature* **395**, 503–507.
46. Xia, X. M., Zeng, X. & Lingle, C. J. (2002) *Nature* **418**, 880–884.
47. Partridge, L. D. & Swandulla, D. (1988) *Trends Neurosci.* **11**.
48. Liman, E. R. (2003) *J. Physiol.* **548**, 777–787.
49. Chuang, H. H., Prescott, E. D., Kong, H., Shields, S., Jordt, S. E., Basbaum, A. I., Chao, M. V. & Julius, D. (2001) *Nature* **411**, 957–962.
50. Prescott, E. D. & Julius, D. (2003) *Science* **300**, 1284–1288.
51. Prawitt, D., Monteilh-Zoller, M. K., Brixel, L., Spangenberg, C., Zabel, B., Fleig, A. & Penner, R. (2003) *Proc. Natl. Acad. Sci. USA* **100**, 15166–15171.